Crystal Structure Theory and Applications, 2015, 4, 1-8
Published Online March 2015 in SciRes. http://www.scirp.org/journal/csta
http://dx.doi.org/10.4236/csta.2015.41001

Metal-Organic Deposition of Epitaxial $La_{0.7}Sr_{0.3}CoO_3$ Thin Films on $LaAlO_3$ Substrates

Kais Daoudi[1,2*], Zied Othmen[2], Saoussen El Helali[3], Meherzi Oueslati[2], Tetsuo Tsuchiya[4]

[1]Department of Applied Physics, College of Sciences, University of Sharjah, Sharjah, UAE
[2]Unité Nanomatériaux et Photonique, Faculty of Sciences of Tunis, Tunis El Manar University, Tunis, Tunisia
[3]Laboratoire de Physico-Chimie des Matériaux, Faculty of Science of Monastir, University of Monastir, Tunis, Tunisia
[4]National Institute of Advanced Industrial Science and Technology (AIST), Tsukuba, Japan
Email: *kais.daoudi@gmail.com

Received 23 February 2015; accepted 13 March 2015; published 18 March 2015

Abstract

$La_{0.7}Sr_{0.3}CoO_3$ (LSCO) thin films were epitaxially grown on (001)-single crystalline $LaAlO_3$ substrates by metal organic deposition. The evolution of the crystallinity of the films having various thicknesses and obtained at various annealing temperatures is investigated using Raman spectroscopy. The Raman mode associated to the Jahn-Teller distortions in the LSCO films is found to be dependent on the annealing temperature and sensitive to the strain state evolution with film thickness. The microstructure and morphology of the obtained films were investigated using transmission electron microscopy observations on cross-sections and atomic force microscopy. The obtained films are characterized by nanocrystalline morphology, with an average roughness around 5 nm. By increasing the annealing temperature to 1000˚C and the film thickness to 100 nm, the electrical resistivity was decreased by several orders of magnitude. The film resistivity reaches approximately 2.7×10^{-4} Ω·cm in a wide interval of temperature of 77 - 320 K, making this material a promising candidate for a variety of applications.

Keywords

$La_{0.7}Sr_{0.3}CoO_3$, Thin Films, MOD, TEM, Raman Spectroscopy, Resistivity

*Corresponding author.

How to cite this paper: Daoudi, K., Othmen, Z., El Helali, S., Oueslati, M. and Tsuchiya, T. (2015) Metal-Organic Deposition of Epitaxial $La_{0.7}Sr_{0.3}CoO_3$ Thin Films on $LaAlO_3$ Substrates. *Crystal Structure Theory and Applications*, **4**, 1-8.
http://dx.doi.org/10.4236/csta.2015.41001

1. Introduction

Strontium-doped lanthanum cobaltite ($La_{1-x}Sr_xCoO_3$: LSCO) has created renewed research interest in the mixed valence transition metal-oxides with perovskite and related structures. Owing to their relatively high electrical [1]-[3] and ionic conductivity [4]-[6], cobaltites in thin film forms have been used in fuel cells, oxygen penetration membranes, and as electrodes in ferroelectric memory technology. The physical properties of LSCO material in bulk form are basically sensitive to the chemical composition [1] [6]. However, when this material is prepared in thin film form, the physical properties are sensitive to structure, oxygen content, and disorder. In particular, the interface between the films and the substrate can play an important role, giving rise to phase-separated regions with different magnetic structures and affecting the transport properties especially in very thin films. Consequently, the growth method, the deposition parameters, and also the substrate-induced strain will influence the electrical and magnetic properties. The epitaxial growth of such cobaltite thin films is increasingly required for several applications. Therefore, the physical properties of the film will be strongly dependent on the preparation route. Actually, the epitaxial growth of various doped cobaltite films is usually done using conventional physical processes, such as pulsed laser deposition (PLD) [7] or sputtering techniques [8], requiring high vacuum and post-annealing. Therefore, to reduce the production cost, preparation of the epitaxial LSCO thin films using a simple process will be appreciated by researchers and engineers. The chemical processes such as sol-gel [8]-[11] or metal organic deposition (MOD) [12] do not require a vacuum system and a complex apparatus which is particularly important for several applications. The MOD process is one of the promising fabrication methods of oxide films, which has great advantages of low fabrication cost, easy stoichiometry control, high deposition rate, and is easily applicable to substrates of any shape and size. In a previous paper we have obtained high-quality epitaxy and promising physical properties of $La_{0.7}Sr0_{0.3}CoO_3$ (LSCO) thin films on $SrTiO_3$ (STO) single crystal substrates [13]. The structural and electrical properties of the LSCO films grown on STO substrates have been investigated and correlated to the substrate-induced strain. The lattice mismatch between the LSCO film and the STO substrate is calculated by $\delta_{STO} = (c_b - c_s)/c_s$, where $c_b = 3.82$ Å is the bulk lattice parameter of the film material and $c_s = 3.905$ Å is the bulk lattice parameter for the STO substrate [7] [14]. The lattice mismatch of the LSCO/STO system is around –2.17% indicating an important in-plane tensile strain in the LSCO film. Therefore, in the present study, the LSCO films were epitaxially grown on the very small lattice-mismatched substrate ($\delta_{LAO} = +0.84\%$) $LaAlO_3$ (LAO) imposing a small compressive strain. The structural, morphology and electrical properties of the LSCO films grown on LAO substrates by MOD process have been discussed.

2. Experimental

The LSCO thin films were prepared by a conventional MOD process. The starting solution was prepared by mixing the constituent metal-naphthenate solution (Nihon Kagaku Sangyo) and diluting with toluene to obtain the required concentration and viscosity. The molar ratios of La, Sr and Co in the coating solution were 0.7, 0.3 and 1.0, respectively. This solution was spin-coated onto (001) single crystal LAO substrates at 4000 rpm for 10 seconds. To eliminate the toluene, the metal-organic (MO) film was then dried in air at 100˚C for 10 min. Before the final annealing, a preheating step at 500˚C for 30 min is necessary to decompose the organic part. The preheating step is also required to prevent the formation of fissures on the film surface during the final thermal annealing at high temperatures. To obtain a satisfactory film thickness, the above procedure (coating, drying, and preheating) was repeated several times (up to 4 - 5 times) giving rise to a corresponding number of superimposed layers in the LSCO product film. The final annealing was carried out in a conventional furnace at 600˚C - 1000˚C for 60 min in air.

The Raman spectra were obtained using a T64000 Jobin-Yvon triple spectrometer, equipped with a liquid nitrogen cooled charge coupled device (CCD) and a microscope. A backscattering geometry was used with the sample placed under the microscope with ×100 magnification lens. The excitation is carried out by a laser wavelength of 488 nm with a power estimated on the film surface around 5 mW. Raman measurements covered the range between 100 and 800 cm^{-1}. The cross-section transmission electron microscopy (XTEM) observations were performed using a high resolution electron Hitachi H-9000 microscope operated at 300 kV. The XTEM specimens were prepared following the conventional method, *i.e.*, mechanical cutting, face-to-face gluing, mechanical grinding, polishing and dimpling, followed by Ar-ion milling at 4 KV. The surface morphology and roughness of the samples were studied by atomic force microscopy (AFM: Nanopics 2100) with the damping

mode. The resistivity-temperature (ρ-T) curves were measured by the usual DC four-probe method and by cooling the samples from 320 K to liquid nitrogen temperature (77 K).

3. Results and Discussion

3.1. Microstructure and Surface Morphology of the Films

Raman spectroscopy is a powerful tool for a study of various vibrational modes and electronic transitions in solids. As well, Raman spectroscopy may be a useful method to follow the crystallinity evolution of freshly grown thin films. Therefore, in order to confirm the absence of secondary phases or microstructural defects by increasing the annealing temperature or film thickness, we carried out detailed micro-Raman spectroscopy measurements. **Figure 1** shows the room temperature Raman spectra of the LAO substrate and the 40 nm-thick LSCO films annealed at various temperatures (800˚C, 900˚C, and 1000˚C).

The Raman spectrum of the LAO substrate is shown as a reference. Three strong modes at 120, 150, and 487 cm^{-1} dominate the Raman spectrum of LAO. Similar results have been obtained by Abrashev *et al.* [15], and more recently by J. Suda *et al.* [16]. The main peaks of the LAO have been assigned to A_{1g} mode at 120 cm^{-1} (rotation of the oxygen octahedra around the hexagonal [001]*h* direction), *Eg* mode at 150 cm^{-1} [pure La vibration in the hexagonal (001)*h* plane] and *Eg* mode at 487 cm^{-1} (pure oxygen bending vibration), respectively. In addition to these strong modes we note in the Raman spectra of LAO, the presence of two broad bands around 280 cm^{-1} and 420 cm^{-1} which have not been observed by Abrashev *et al.* [15].

In this study we are focusing mainly on the LSCO films, therefore, deep discussions of the LAO vibrational properties are necessary and will be reported in the future. After deposition of 40-nm thick LSCO film on the LAO substrate, we can easily distinguish a Raman mode at 695 cm^{-1}, which is due to the Co-O bending vibration [17]. The 695 cm^{-1} peak intensity increases with an increase in the annealing temperature from 800˚C to 1000˚C indicating an improvement of the film crystallinity. In fact, at 1000˚C in annealing temperature, the 695 cm^{-1} peak have the highest intensity and the lowest full width at half maximum (FWHM). We note also the presence at 1000˚C, and not at low annealing temperatures (800˚C and 900˚C), of a Raman mode at 525 cm^{-1}. The 525 cm^{-1} and 695 cm^{-1} modes are typical characteristics of the Jahn-Teller distortion in the LSCO material. Therefore, at this “optimal” annealing temperature (1000˚C), we varied the film thickness in order to survey the strain relaxation effects on the structural and electrical properties of these LSCO films.

The Raman spectra evolution with film thickness is presented in **Figure 2**. For the 20 nm thick film, the Raman signature is not easily distinguished from that one of the LAO substrate. In fact, the LSCO signature is evidenced by a broad band with a very low intensity observed around the 695 cm^{-1} peak. By increasing the film

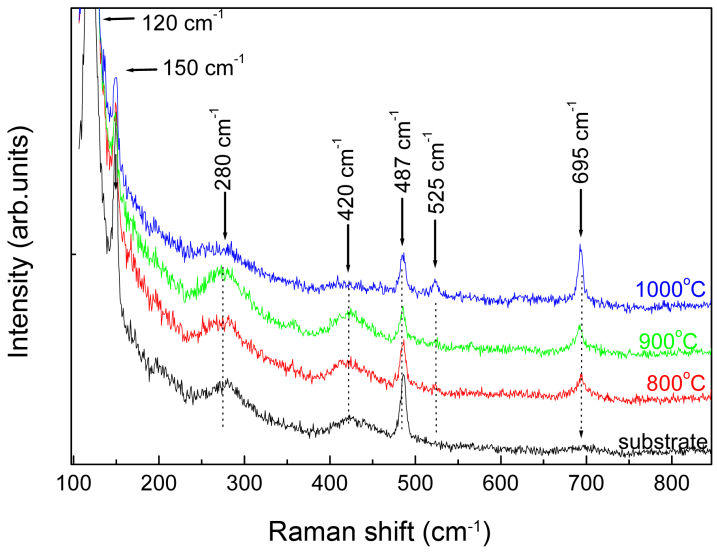

Figure 1. Room-temperature Raman spectra of the LAO substrate and the 40 nm-thick LSCO films grown on LAO using MOD process at various annealing temperatures (800˚C - 1000˚C).

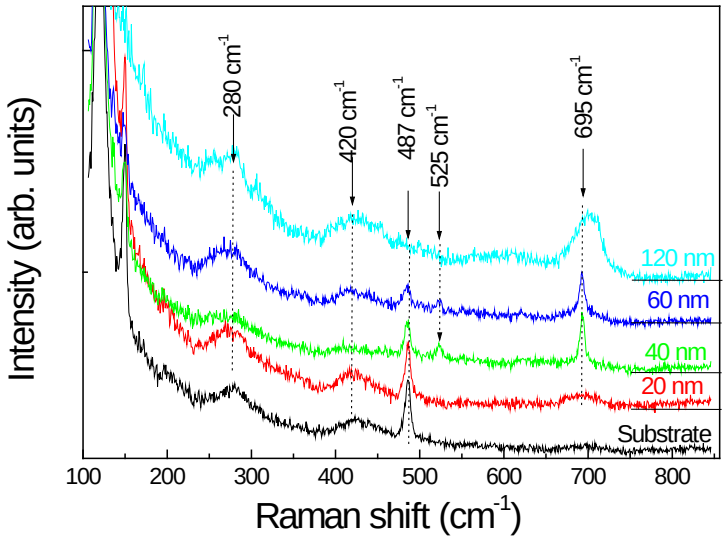

Figure 2. Variation of the room-temperature Raman spectra vs. thickness of the LSCO films grown on LAO substrates using MOD process with a thermal annealing at 1000˚C.

thickness to 40 and 60 nm, the 695 cm^{-1} peak's intensity is remarkably increased. The 525 cm^{-1} mode is only distinguished for the 40 nm thick film. By increasing the film thickness the Raman signature of the LSCO/LAO system becomes dominated by that one of the film. In fact over 60 nm in film thickness we note an important broadening of the 695 cm^{-1} mode for the 120 nm thick film. The thicker film (120 nm) is totally relaxed and may probably contain microstructural defects compared to the strained thin ones. The Raman modes of LAO are hardly distinguished from those of the 120 nm thick LSCO film.

Figure 3 shows cross-sectional TEM image of the LSCO thin film grown on LAO substrate by the MOD process with a thermal annealing at 1000˚C for 60 min in air. TEM observations were performed on a cross-section specimen along the $<100>_{LAO}$ zone axis.

The LSCO film shown in **Figure 3(a)** is composed of two deposited layers. As can be seen in **Figure 3(a)**, the film exhibits good homogeneity in depth without interfaces between the layers or granular structures. From the XTEM images (**Figure 3(a)**), the film thickness is precisely measured. The two-layer film is approximately 40 nm thick. Therefore, one deposited layer by the MOD of LSCO is approximately 20 nm. Using the MOD process for the epitaxial growth of $La_{0.7}Ca_{0.3}MnO_3$ (LCMO) we found similar film thickness [18]. The corresponding selected area electron diffraction (SAED) pattern is shown in **Figure 3(b)**, indicating a (001) epitaxial growth of the LSCO film on the LAO substrate. The high-resolution TEM image (**Figure 1(c)**) confirms the (001) epitaxial growth of the LSCO film and reveals a good homogeneity without specific dislocations or strained zones. The lattice mismatch can be accommodated either by straining the lattices or by the formation of misfit dislocations at the interface depending on the elastic properties of the materials and the film thickness. The in-plane lattice mismatch between the LSCO film and the LAO substrate is around +0.84%. Hence, using the cross-section HRTEM observations along the LSCO/LAO interface, we noted a good epitaxy throughout the entire film without dislocations (**Figure 3(c)**). We note also a good interface between the LSCO film and the LAO substrate. This is a proof of the absence of a kind chemical reaction which may probably happen during the thermal annealing at a relatively high temperature (1000˚C).

Using chemical processes such as MOD or sol-gel, the film roughness is usually higher than that one produced by physical processes such as pulsed laser deposition (PLD) or molecular beam epitaxy (MBE). Hence, we showed in **Figure 4**, the 3D AFM images of the 20 nm (a), 40 nm (b) and 60 nm (c) thick LSCO films produced by MOD and annealed at 1000˚C. As can be seen in **Figure 4**, an island growth surface morphology was observed for various films.

The root-mean-square (rms) values of roughness for the 20, 40 and 60 nm-films are 3.7 nm, 4.3 and 5.2 nm, respectively. These rms values are little bit higher than those of LCMO thin films grown on LAO substrates by MOD [19], were the rms values have been found around 3 nm. The rms value of the $La_{0.5}Sr_{0.5}CoO_3$ films pre-

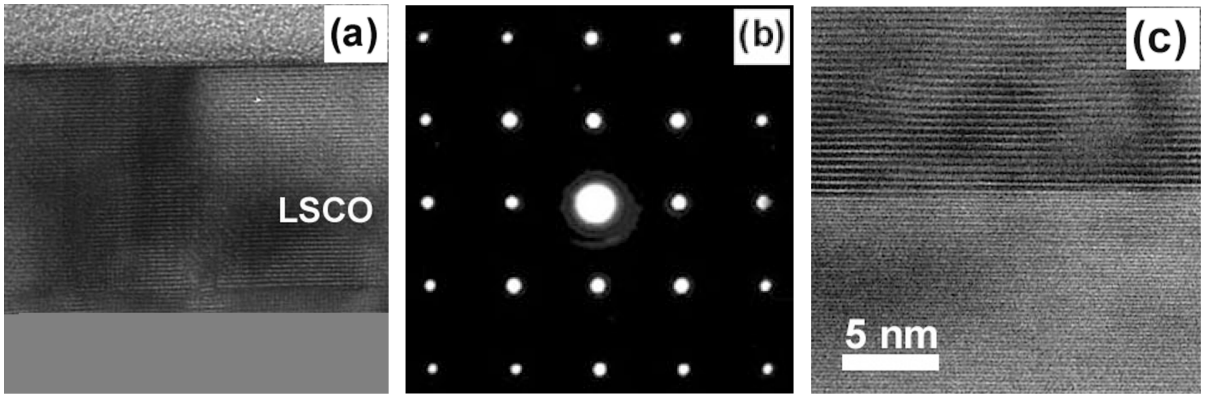

Figure 3. (a) Low magnification XTEM image, SAED pattern (b), and HRTEM image (c) of the two-layer LSCO film grown on LAO substrate by MOD at 1000˚C.

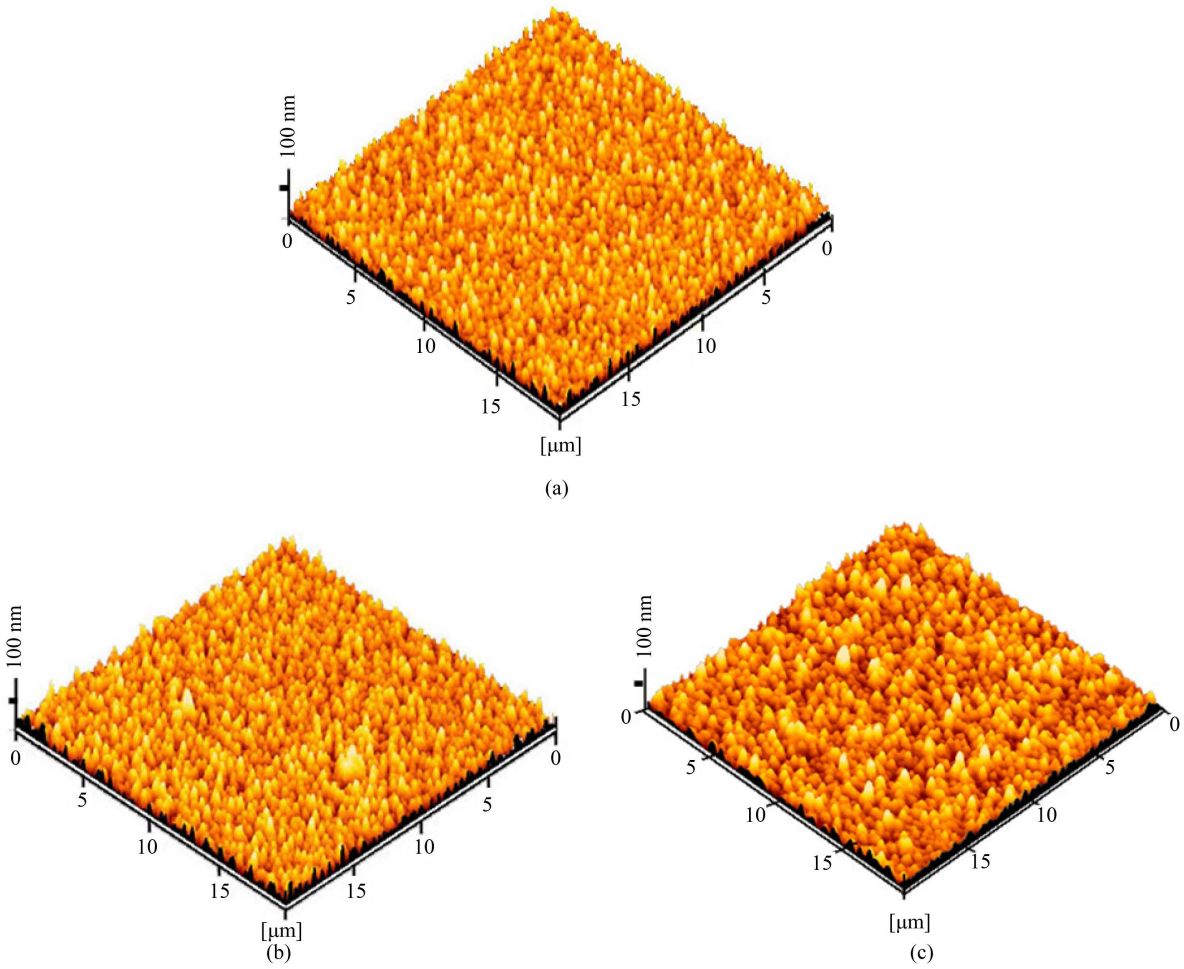

Figure 4. 3D-AFM images of LSCO films having different thicknesses; 20 nm (a), 40 nm (b), and 60 nm (c), deposited on LAO substrates by MOD with a thermal annealing at 1000˚C.

pared by PLD process on LAO substrates are around 0.5 nm [20]. $La_{0.8}Sr_{0.2}CoO_3$ prepared by PLD process on yttria-stabilized zirconia (YSZ) single crystals substrates exhibited rms value in the interval 0.71 - 1.32 nm [21]. After a thermal annealing at 900˚C of the $Nd_{0.8}Sr_{0.2}CoO_3$ films produced by radio-frequency magnetron sputtering [22], the rms reaches 50 nm, which is much larger than those exhibited by our films produced by MOD

process. Hence, the MOD technique based on spin-coating of the starting metal-organic solution, followed by a thermal annealing looks much better in terms of film surface than the sputtering process.

3.2. Electrical Properties

In order to characterize the electrical properties of our films in more detail, we carried out transport measurements as a function of temperature. **Figure 5** shows the variation of the electrical resistivity of the 100 nm-thick LSCO films grown on LAO substrates using the MOD process at various thermal annealing temperatures (600˚C - 1000˚C). The LSCO film annealed at 600˚C shows a semiconducting like behavior ($\frac{d\rho}{dT} < 0$) over the entire temperature range studied.

The semiconducting behavior of this film is likely due to oxygen deficiency. Ebenso *et al*. [23] reported similar results concerning the LSCO films prepared by spray pyrolysis process and attributed the semiconducting behavior to the oxygen deficiency. By increasing the annealing temperature from 600˚C to 800˚C we note an important decrease of the resistivity within all the large interval of temperature (80 - 320 K). This is due to an improvement in the oxygen content and the crystallinity of the LSCO films. The semiconducting behavior over the entire range of temperature obtained for the film annealed at 600˚C disappears at an annealing temperature higher than 800˚C, and a kind of a ferromagnetic transition is barely distinguished.

An increase in the film thickness is usually followed by a strain relaxation and therefore a change in electrical transport. By increasing the thickness from 20 to 100 nm for the LSCO films grown by MOD at 1000˚C, a noticeable decrease in the resistivity is obtained (**Figure 6**).

The 20 nm thick-film annealed at 1000˚C exhibit a semiconducting-like behavior in the whole temperature interval. However, the 20 and 40 nm thick-LSCO films grown on STO substrates exhibit the semiconducting behavior [13]. This might be due to the differences in the lattices mismatches between the LSCO and the LAO (+0.84%) and STO (−2.17%). In fact an increase in the lattice mismatch in absolute value is usually followed by an increase in the critical film thickness for strain relaxation. Therefore, for 40 nm thick-LSCO film grown on LAO substrate, the strain is much lower than that one in the film grown STO substrate. Over 40 nm in film thickness, the LSCO exhibited a usual cobaltite ρ(T) curves characterized by a broad transition from a metallic state to a semiconducting state. An increase in the film thickness from 20 to 100 nm is followed by a decrease in the film resistivity from 10×10^{-3} Ω·cm to 4×10^{-4} Ω·cm at 300 K. The 100 nm thick-LSCO film annealed at 1000˚C is characterized by a rather constant resistivity of $(2.7 - 4) \times 10^{-4}$ Ω·cm in the whole temperature interval between 77 and 320 K. The absence of easily distinguished ferromagnetic transition and the relatively

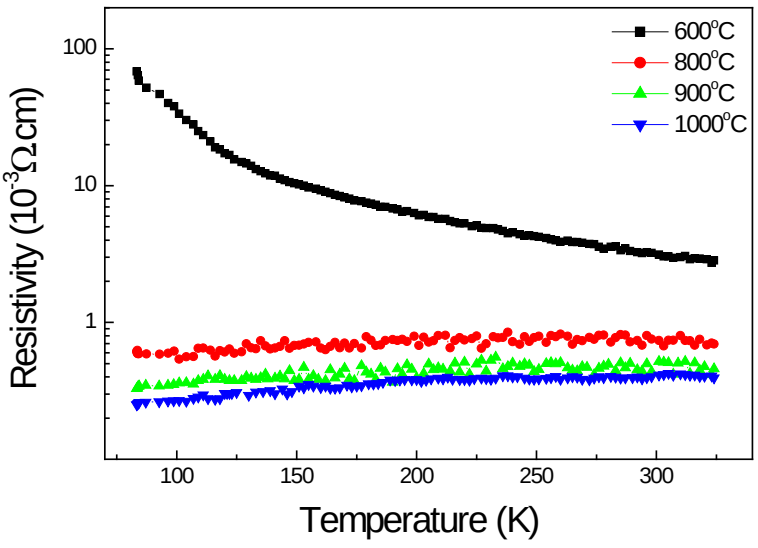

Figure 5. Temperature dependence of resistivity for the 100 nm-thick LSCO films grown on LAO substrates by MOD process at different annealing temperatures (600˚C - 1000˚C).

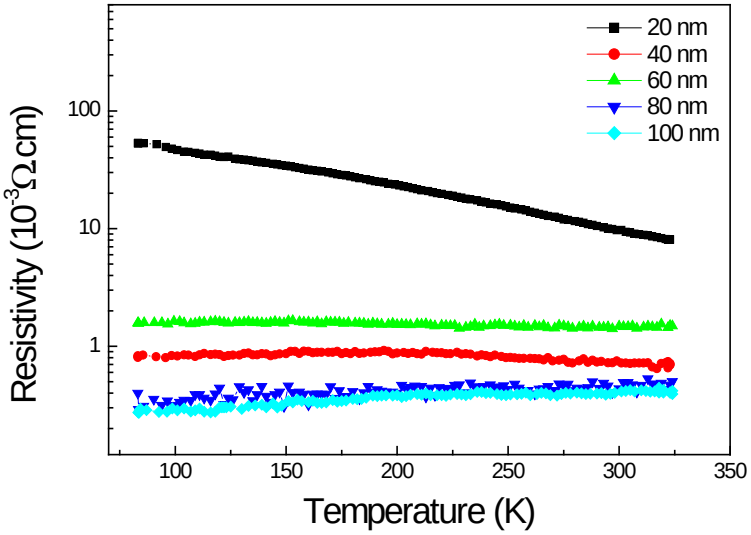

Figure 6. Temperature dependence of resistivity for the LSCO films with various thicknesses (20 - 100 nm) grown on LAO substrates by MOD with a thermal annealing at 1000˚C.

low values of resistivity, when compared to the same films grown for example by PLD process, are probably due to the presence of amorphous phases, oxygen deficiency, and defects.

4. Conclusion

Using a simple and low-cost metal-organic deposition process, we have prepared epitaxial LSCO thin films on LAO substrates. The film thicknesses have been precisely measured through TEM observations on cross-sections. The LSCO/LAO interfaces are found to be sharp and easily distinguished. The obtained films have an acceptable roughness (3 - 4 nm) for further integration, for example, in multilayered structures. The Raman mode associated to the Jahn-Teller distortions is found to be strongly dependent on the oxygen stoichiometry and thickness of the LSCO film. The electrical resistivity values are rather constant in a wide temperature interval between 77 and 300 K for the totally relaxed films with a thickness over 40 nm.

References

[1] Mizusaki, J., Tabuchi, J., Matsuura, T., Yamauchi, S. and Fueki, K. (1989) Electrical Conductivity and Seebeck Coefficient of Nonstoichiometric $La_{1-x}Sr_xCoO_{3-\delta}$. *Journal of the Electrochemical Society*, **136**, 2082. http://dx.doi.org/10.1149/1.2097187

[2] Mineshige, A., Inaba, M., Yao, T., Ogumi, Z., Kikiuchi, K. and Kawase, M. (1996) Crystal Structure and Metal-Insulator Transition of $La_{1-x}Sr_xCoO_3$. *Journal of Solid State Chemistry*, **121**, 423. http://dx.doi.org/10.1006/jssc.1996.0058

[3] Senaris-Rodriguez, M.A. and Goodenough, J.B. (1995) Magnetic and Transport Properties of the System $La_{1-x}Sr_xCoO_{3-\delta}$ ($0 < x \leq 0.50$). *Journal of Solid State Chemistry*, **118**, 3238. http://dx.doi.org/10.1006/jssc.1995.1351

[4] Ohno, Y., Nagata, S. and Sato, H. (1983) Properties of Oxides for High Temperature Solid Electrolyte Fuel Cell. *Solid State Ionics*, **9**, 1001. http://dx.doi.org/10.1016/0167-2738(83)90122-4

[5] Ishigaki, T., Yamauchi, S., Mizusaki, J., Fueki, K. and Tamura, H. (1984) Tracer Diffusion Coefficient of Oxide Ions in $LaCoO_3$ Single Crystal. *Journal of Solid State Chemistry*, **54**, 100. http://dx.doi.org/10.1016/0022-4596(84)90136-1

[6] Kharton, V.V., Naumovich, E.N., Vecher, A.A. and Nicolaev, A.V. (1995) Oxide Ion Conduction in Solid Solutions $Ln_{1-x}Sr_xCoO_{3-\delta}$ (Ln = La, Pr, Nd). *Journal of Solid State Chemistry*, **120**, 128. http://dx.doi.org/10.1006/jssc.1995.1387

[7] Rata, A.D., Herklotz, A., Nenkov, K., Schultz, L. and Dorr, K. (2008) Strain-Induced Insulator State and Giant Gauge Factor of $La_{0.7}Sr_{0.3}CoO_3$ Films. *Physical Review Letters*, **100**, Article ID: 076401. http://dx.doi.org/10.1103/PhysRevLett.100.076401

[8] Torija, M.A., Sharma, M., Fitzsimmons, M.R., Varela, M. and Leighton, C. (2008) Epitaxial $La_{0.5}Sr_{0.5}CoO_3$ Thin Films: Structure, Magnetism, and Transport. *Journal of Applied Physics*, **104**, Article ID: 023901.

http://dx.doi.org/10.1063/1.2955725

[9] Popa, M. and Moreno, J.M.C. (2009) Lanthanum Cobaltite Thin Films on Stainless Steel. *Thin Solid Films*, **517**, 1530. http://dx.doi.org/10.1016/j.tsf.2008.08.187

[10] Armelao, L., Barreca, D., Bottaro, G., Gasparotto, A., Maragno, C. and Tondello, E. (2005) Hybrid Chemical Vapor Deposition/Sol-Gel Route in the Preparation of Nanophasic $LaCoO_3$ Films. *Chemistry of Materials*, **17**, 427. http://dx.doi.org/10.1021/cm0489643

[11] Tealdi, C., Saiful Islam, M., Fisher, C.A.J., Malavasi, L. and Flor, G. (2007) Defect and Transport Properties of the $NdCoO_3$ Catalyst and Sensor Material. *Progress in Solid State Chemistry*, **35**, 491-499. http://dx.doi.org/10.1016/j.progsolidstchem.2007.01.015

[12] Manabe, T., Kondo, W., Mizuta, S. and Kumagai, T. (1992) Preparation of Superconducting $Ba_2YCu_3O_{7-y}$-Ag Composite Films on Sapphire by the Dipping Pyrolysis Process. *Applied Physics Letters*, **60**, 3301. http://dx.doi.org/10.1063/1.106696

[13] Daoudi, K., Tsuchiya, T., Nakajima, T., Fouzri, A. and Oueslati, M. (2010) Epitaxial Growth of $La_{0.7}Sr_{0.3}CoO_3$ Thin Films on $SrTiO_3$ Substrates by Metal-Organic Deposition. *Journal of Alloys and Compounds*, **506**, 483-487. http://dx.doi.org/10.1016/j.jallcom.2010.07.035

[14] Caciuffo, R., Rinaldi, D., Barucca, G., Mira, J., Rivas, J., Rodriguez, M.A.S., Radaelli, P.G., Fiorani, D. and Goodenough, J.B. (1999) Structural Details and Magnetic Order of $La_{1-x}Sr_xCoO_3$ ($x < \sim 0.3$). *Physical Review B*, **59**, 1068. http://dx.doi.org/10.1103/PhysRevB.59.1068

[15] Abrashev, M.V., Litvinchuk, A.P., Iliev, M.N., Meng, R.L., Popov, V.N., Ivanov, V.G., Chakalov, R.A. and Thomsen, C. (1999) Comparative Study of Optical Phonons in the Rhombohedrally Distorted Perovskites $LaAlO_3$ and $LaMnO_3$. *Physical Review B*, **59**, 4146. http://dx.doi.org/10.1103/PhysRevB.59.4146

[16] Suda, J., Kamishima, O., Kawamura, J., Hattori, T. and Sato, T. (2009) Anharmonicity on Raman Active Phonon Modes of $LaAlO_3$. *Journal of Physics*: *Conference Series*, **150**, Article ID: 052249. http://dx.doi.org/10.1088/1742-6596/150/5/052249

[17] Orlovskaya, N., Steinmetz, D., Yarmolenko, S., Pai, D., Sankar, J. and Goodenough, J. (2005) Detection of Temperature- and Stress-Induced Modifications of $LaCoO_3$ by Micro-Raman Spectroscopy. *Physical Review B*, **72**, Article ID: 014122. http://dx.doi.org/10.1103/PhysRevB.72.014122

[18] Daoudi, K., Tsuchiya, T., Yamaguchi, I., Manabe, T., Mizuta, S. and Kumagai, T. (2005) Microstructural and Electrical Properties of $La_{0.7}Ca_{0.3}MnO_3$ Thin Films Grown on $SrTiO_3$ and $LaAlO_3$ Substrates Using Metal-Organic Deposition. *Journal of Applied Physics*, **98**, Article ID: 013507. http://dx.doi.org/10.1063/1.1943514

[19] Daoudi, K., Tsuchiya, T., Mizuta, S., Yamaguchi, I., Manabe, T. and Kumagai, T. (2004) Large Temperature Coefficient of Resistance in $La_{0.7}Ca_{0.3}MnO_3$ Thin Films Obtained by Metal Organic Deposition Process. *Japanese Journal of Applied Physics*, **43**, Article ID: L1054.

[20] Chen, X., Wang, S., Yang, Y.L., Smith, L., Wu, N.J., Kim, G.-I., Perry, S.S., Jacobson, A.J. and Ignatiev, A. (2002) Electrical Conductivity Relaxation Studies of an Epitaxial $La_{0.5}Sr_{0.5}CoO_{3-\delta}$, Thin Film. *Solid State Ionics*, **146**, 405-413. http://dx.doi.org/10.1016/S0167-2738(01)01031-1

[21] Mori, D., Oka, H., Suzuki, Y., Sonoyama, N., Yamada, A., Kanno, R., Sumiya, Y., Imanishi, N. and Takeda, Y. (2006) Synthesis, Structure, and Electrochemical Properties of Epitaxial Perovskite $La_{0.8}Sr_{0.2}CoO_3$ Film on YSZ Substrate. *Solid State Ionics*, **177**, 535-540. http://dx.doi.org/10.1016/j.ssi.2005.12.032

[22] Malavasi, L., Quartarone, E., Sanna, C., Lampis, N., Lehmann, A.G., Tealdi, C., Mozzati, M.C. and Flor, G. (2006) Radio Frequency Sputter Deposition of Epitaxial Nanocrystalline $Nd_{1-x}Sr_xCoO_3$ Thin Films. *Chemistry of Materials*, **18**, 5230-5237. http://dx.doi.org/10.1021/cm061420b

[23] Ebenso, E.E., Sardar, K., Chandrasekhar, M., Raju, A.R. and Rao, C.N.R. (2000) Thin Films of $Ln_{1-x}Sr_xCoO_3$ (Ln = La, Nd and Gd) and $SrRuO_3$ by Nebulized Spray Pyrolysis. *Solid State Sciences*, **2**, 833-839. http://dx.doi.org/10.1016/S1293-2558(00)01098-0